



Thermoelectric properties of Cu-added Zn–Sb based alloys with multi-phase equilibrium

J.L. Cui^{a,*}, H. Fu^b, D.Y. Chen^b, L.D. Mao^c, X.L. Liu^a, W. Yang^a

^aSchool of Mechanical Engineering, Ningbo University of Technology, Ningbo, 315016, China

^bSchool of Materials Science and Engineering, China University of Mining and Technology, Xuzhou, 221008, China

^cCollege of Chemical Engineering and Materials Science, Zhejiang University of Technology, Hangzhou, 310014, China

ARTICLE DATA

Article history:

Received 24 November 2007

Received in revised form

23 January 2009

Accepted 23 January 2009

PACS:

60

70

Keywords:

Cu-added Zn–Sb based alloys

Multi-phase structures

Thermoelectric properties

ABSTRACT

The polycrystalline samples of Cu-added Zn–Sb based alloys with multi-phase equilibrium were prepared by spark plasma sintering and their microstructures and thermoelectric properties were evaluated. After Cu addition into Zn–Sb based alloys we observed a major phase ZnSb, β -Zn₄Sb₃, the second phase Cu₂Sb and remnant Zn. The ZnSb phase plays an important role in increasing Seebeck coefficient (α) and decreasing electrical conductivity (σ), and Cu₂Sb is of significance to the improvement of the thermoelectric performance. The thermal conductivities (κ) increase with Cu content, and are almost independent of temperature below 574 K. If in comparison with the highest ZT value (ZT=0.48, at 654 K) of Zn₄Sb₃ prepared in the present work, we obtain the value of 0.7 for the alloy with a certain Cu concentration at the corresponding temperature.

© 2009 Elsevier Inc. All rights reserved.

1. Introduction

β -Zn₄Sb₃, one of the stable compounds used in intermediate temperatures, has attracted a lot of interest as a thermoelectric material due to its low lattice thermal conductivity. However, since the evaporation of element Zn during sintering, pure β -Zn₄Sb₃ phase cannot easily be obtained, and multi-phase structures, which include β -Zn₄Sb₃, ZnSb and remnant Zn, are usually observed [1,2]. To date, many studies with respect to Zn–Sb based alloys such as phase diagram [3,4], physical properties [5,6] and microstructures [7] have been conducted, but little attention has been paid to the effects of phases on the thermoelectric properties.

Recent works in our group reveal that an addition of Ag/Cu or their compounds with determined concentration in the p-type Bi–Te based alloys can greatly improve thermoelectric perfor-

mance [8–10], because one of the key points is that there are precipitated metallic phases and possible existence of nanostructures that can reduce lattice thermal conductivities. On one hand, Zn–Sb based alloys are a kind of materials with higher level of atomic disorder and hole concentration, discovered disorder in β -Zn₄Sb₃ manifests in the framework Zn position, which displays a considerable occupational deficiency (0.89–0.90) and in the occurrence of three weakly occupied (by around 0.06) general positions representing interstitial Zn atoms [7]. Therefore, unlike those in the Bi–Te based alloys, only limited doping effect can be expected. On the other hand, however, ZnSb is also known as a thermoelectric (TE) material with larger Seebeck coefficients and higher thermal conductivities than typical semiconductor β -Zn₄Sb₃ does [11–13], if a foreign element is doped into the Zn–Sb based alloys, the effects of formed ZnSb and other precipitated metallic phases on the

* Corresponding author. Tel./fax: +86 574 87081258.

E-mail address: cuijl@nbip.net (J.L. Cui).

modulation of transport properties should be very important. Considering the fact that elements Cd and In have more valence electrons than Cu and Ag, it is presumed that an incorporation of Cu in the Zn–Sb based alloys can produce more hole concentration, which may effectively optimize the carrier concentration. In addition, an atomic radius of Cu (1.57×10^{-10} m) is smaller than those of Cd (1.71×10^{-10} m) and In (2.0×10^{-10} m) [14], Cu could readily interstitially occupy the gaps in the Zn–Sb lattice, which enhances the lattice distortion and reduces the lattice thermal conductivity. Therefore, an addition of Cu in the Zn_4Sb_3 based alloys could be of great significance to the improvement of TE properties.

In the present work, Cu-added Zn–Sb based alloys with multi-phase equilibrium were prepared and their microstructures and TE properties were evaluated.

2. Experimental

Polycrystalline samples were prepared according to the formula $\text{Zn}_{4-x}\text{Cu}_x\text{Sb}_3$ ($x=0-0.4$) by melting the mixtures composed of high purity (5 N) elements Zn, Sb and Cu in evacuated quartz tubes at 1323 K for 10 h. During melting 30-s rocking every 1 h was conducted to ensure that the composition was homogenous without segregation. After quenching in water the ingots were ball-milled for 5 h in stainless steel bowls with a rotation rate of 350 rpm. The sintering of the powders was carried out with spark plasma sintering apparatus (SPS-1030) using a pre-designed sintering program at a pressure of 40 MPa and 723 K. In order to avoid Zn evaporation from the crystals during sintering [15], a relatively rapid sintering process was recommended with the heating and holding time each of only 5 min. The subsequent heat treatment was conducted for the compacts in vacuum at 453 K for 10 h to ensure homogeneity and to eliminate the internal stress as much as possible. The densities of the samples, measured using an Archimedes method, are in a

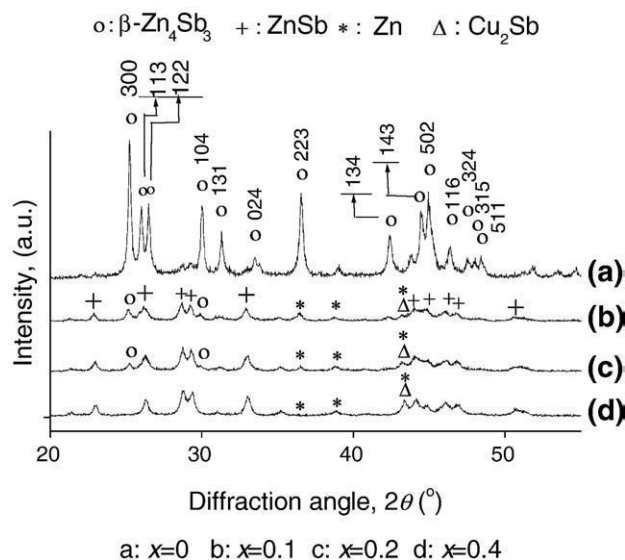


Fig. 1 – X-ray diffraction patterns of the Cu-added $\text{Zn}_{4-x}\text{Cu}_x\text{Sb}_3$ ($x=0-0.4$) alloys.

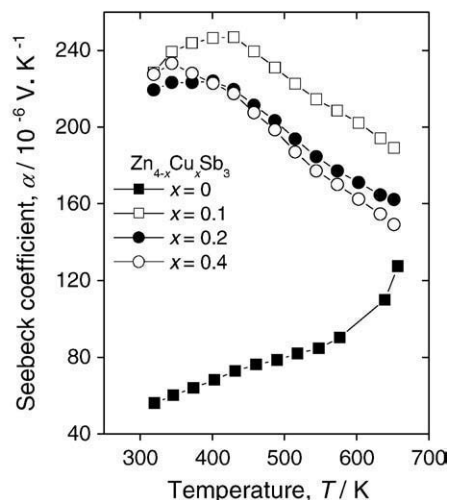


Fig. 2 – The relationship between temperature and Seebeck coefficients for different $\text{Zn}_{4-x}\text{Cu}_x\text{Sb}_3$ ($x=0-0.4$) alloys prepared by spark plasma sintering.

range from 6.09×10^3 to 6.23×10^3 kg/m³. Finally, each sample was cut into 3 mm slices measuring 2.5 mm × 13 mm from the heat treated compacts with the size of ϕ 20 mm × 2.5 mm for property measurements.

The phase structures were investigated by X-ray diffraction (XRD) with a Rigaku D/MAX-2550P diffractometer using Cu K α radiation ($\lambda=0.15406$ nm), using a scan rate of 4° min^{-1} to record the patterns in the 2θ range from 10 to 100° . Rietveld analyses were performed to determine the atomic incorporation in the Zn–Sb sublattice. The Seebeck coefficients (α) and electrical conductivities (σ) were measured using an apparatus (ULVAC ZEM-2) in a helium atmosphere. Thermal diffusivities were measured by a laser flash method (TC-7000H), and thermal conductivities were calculated from the values of density, specific heat and thermal diffusivity. The Hall coefficients for different samples were measured using an apparatus (HT-648) at 318 K, and the carrier concentrations and mobility were determined using measured electrical conductivities and Hall coefficients.

3. Results and Discussion

3.1. Microstructures

Fig. 1 is the XRD patterns of the Cu-added Zn–Sb based ($x=0-0.4$) samples, indicating that there is a great difference between the profiles for the undoped and Cu-added alloys. The alloy without Cu addition is a $\beta\text{-Zn}_4\text{Sb}_3$ single phase (JCPDS 89-1969) [16] with high peak intensities in the main crystal planes, whereas Cu-added alloys shows only weakened peaks, implying that the grain growth is greatly suppressed after Cu addition. The Cu-added alloys are of structures with multi-phase equilibrium, the structures including a major phase ZnSb (JCPDS 65-2408) [16], small quantities of $\beta\text{-Zn}_4\text{Sb}_3$, Cu_2Sb (JCPDS 65-2815) [16] and remnant Zn (JCPDS 65-5973) [16]. The $\beta\text{-Zn}_4\text{Sb}_3$ phase only occurs in the samples with low content of Cu ($x \leq 0.2$), it

Table 1 – The carrier concentrations and Hall mobility obtained near 318 K for the Cu-added Zn–Sb based alloys $\text{Zn}_{4-x}\text{Cu}_x\text{Sb}_3$ ($x=0-0.4$).

Samples with x	Carrier concentrations (cm^{-3}) near 318 K	Hall mobility (cm^2/Vs) near 318 K
0	8.87×10^{19}	67.4
0.1	3.12×10^{19}	4.93
0.2	3.76×10^{19}	9.70
0.4	4.12×10^{19}	9.48

disappears at $x=0.4$, the peak intensity of Cu_2Sb tends to increase with the starting Cu content, suggesting that the element Cu could not totally dissolve into the Zn–Sb alloy. After close Rietveld analysis to the specimens, we did not find any incorporation of element Cu into the Zn–Sb sublattice, which is inconsistent with the previous expectation, indicating that most Cu atoms were formed in Cu_2Sb compound. The peak intensities of remnant Zn become weaker with Cu content increasing.

3.2. Thermoelectric Properties

After Cu addition into the Zn–Sb based alloys, the α values are significantly increased (Fig. 2), and the maximum α value is 246.9 ($\mu\text{V}/\text{K}$) for $x=0.1$ at 430 K, much higher than that of the $\beta\text{-Zn}_4\text{Sb}_3$ with the maximum α value of 127.5 ($\mu\text{V}/\text{K}$). There are two factors that influence the Seebeck coefficient, scatter factor s and carrier concentration n , according to the expression: $\alpha = \frac{k_B}{e} \left[s + \frac{5}{2} + \ln \frac{2(2\pi m^* k_B T)^{3/2}}{nh^3} \right]$ [17]. We calculated carrier concentrations and mobility using measured Hall coefficients for different samples near 318 K, and observed a markedly decreased Hall mobility and carrier concentration for the Cu-added alloys, as shown in Table 1. Since there are several phases in the Cu-added alloys, complex structures can cause an enhancement of carrier scattering, leading to the increase in scattering factor s . We therefore consider that in the present work both the increased

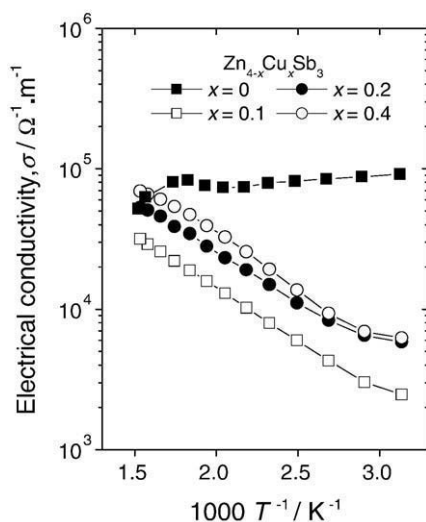


Fig. 3 – The dependence of electrical conductivities on temperature for different $\text{Zn}_{4-x}\text{Cu}_x\text{Sb}_3$ ($x=0-0.4$) alloys prepared by spark plasma sintering.

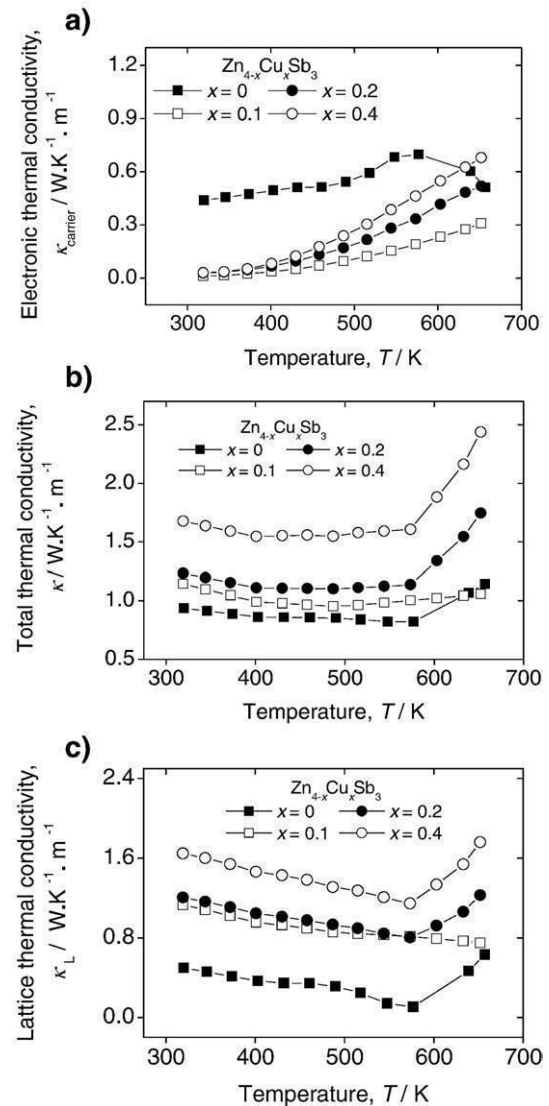


Fig. 4 – The temperature dependence of thermal conductivities for different $\text{Zn}_{4-x}\text{Cu}_x\text{Sb}_3$ ($x=0-0.4$) alloys prepared by spark plasma sintering, (a) $\kappa_{\text{carrier}}-T$, (b) $\kappa-T$, (c) κ_L-T .

scatter factor s and carrier concentration n controls the α values. With the increasing of the Cu_2Sb content the Seebeck coefficient and electrical resistivity tend to decrease, we presume that this metallic phase is of significance to the contribution of free carrier concentration. Contrary to the dependence of Seebeck coefficient, we observed a noticeable decrease of the electrical conductivities (σ) at low temperatures, as shown in Fig. 3. Similarly, this decrease of σ is also attributed to the substantial reduction in mobility μ and n (Table 1). Because the quantity of ZnSb phase takes a large proportion in the present alloys, this major phase was reported to have a higher electrical resistivity ($1.1 \times 10^{-4} \Omega \text{ m}$), Seebeck coefficient (196 $\mu\text{V}/\text{K}$) and much lower hole concentration ($6.3 \times 10^{-24} \text{ m}^{-3}$) at room temperature (R.T.) than $\beta\text{-Zn}_4\text{Sb}_3$ ($2.2 \times 10^{-5} \Omega \text{ m}$, 115 $\mu\text{V}/\text{K}$ and $6.8 \times 10^{-25} \text{ m}^{-3}$, respectively) does [13], therefore, the ZnSb phase plays an important role in controlling the transport data in the present materials.

The temperature dependences of thermal conductivities (κ), electronic component (κ_{carrier}) and lattice contribution (κ_L)

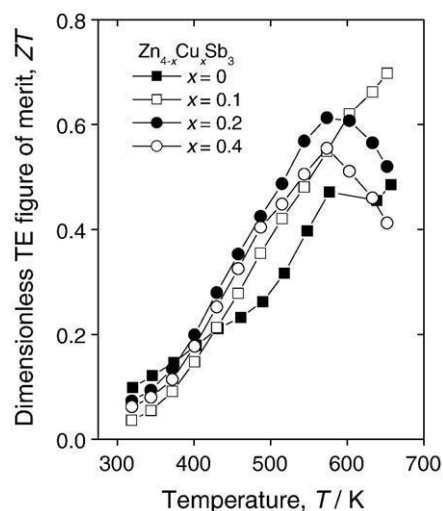


Fig. 5 – The temperature dependence of dimensionless TE figure of merit ZT for different $Zn_{4-x}Cu_xSb_3$ ($x=0-0.4$) alloys.

are shown in Fig. 4. The κ_{carrier} values are estimated from the Wiedemann–Franz law as $\kappa_{\text{carrier}} = LT\sigma$ (Fig. 4a), where L is taken to be $1.5 \times 10^{-8} \text{ V}^2\text{K}^{-2}$ [18], T is absolute temperature. The κ values enhance with starting Cu content, and keep relatively constant below 574 K (Fig. 4b). At $x=0.1$ the κ values are very close to those for the undoped β - Zn_4Sb_3 over the entire temperature range, and are 1.14 (W/mK) and 1.05 (W/mK) at R.T. and 654 K, respectively. The alloy at $x=0.4$ has higher κ values than others for the corresponding temperatures, but still remain similar temperature dependence. The Cu-contained alloys have higher κ_L values than β - Zn_4Sb_3 does (Fig. 4c), the reason is that the κ_L values of ZnSb are much higher than those of β - Zn_4Sb_3 [13]. A typical data can confirm this point, for example, the κ_L value of ZnSb is 2.26 (W/mK) at R.T., whereas that of β - Zn_4Sb_3 is 0.74 (W/mK) [13]. The lattice thermal conductivities for the Cu-added alloys enhance with the Cu_2Sb content, which might mainly be ascribed to the higher κ_L values of the ZnSb itself. A rapid enhancement with temperature for the κ_L values above 574 K might be resulted from an ambipolar contribution.

ZT is defined as $ZT = \alpha^2 \sigma T / \kappa$, the resulting ZT s are shown in Fig. 5. There is a big improvement in ZT over present β - Zn_4Sb_3 , the maximum ZT value of 0.70 is achieved for the Cu-added alloys with $x=0.1$ at 654 K, about 0.22 higher than that of the present β - Zn_4Sb_3 at the corresponding temperature. Therefore, the TE properties of Zn–Sb based alloys can simply be improved by adding a small amount of cheap Cu element, and the second phase Cu_2Sb with proper concentration is of significance to the improvement of the thermoelectric performance for the Zn–Sb based alloys.

4. Conclusion

After addition of Cu into the Zn–Sb based alloys, multi-phase structures can be obtained, the major phase ZnSb plays an important role in determining the transport properties, the

second phase Cu_2Sb , which increases with starting Cu content, is of significance to the improvement of the TE performance. The maximum ZT value of 0.70 is achieved for the alloy with a certain Cu concentration at 654 K, about 0.22 higher than that of the present β - Zn_4Sb_3 at the corresponding temperature.

Acknowledgements

The work was supported by the National Natural Science Foundation of China, Grant No.50871056 and Link Project with Israel (ALIS) (2007B10020).

REFERENCES

- [1] Ur SC, Nash P, Kim Il H. Thermoelectric properties of Zn_4Sb_3 processed by sinter-forging. *Mater Lett* 2004;58:2937–41.
- [2] Ur SC, Nash P, Kim Il H. Mechanical alloying and thermoelectric properties of Zn_4Sb_3 . *J Mater Sci* 2003;38:3553–8.
- [3] Record MC, Izard V, Bulanova M, Tedenac JC. Phase transformation in the Zn–Cd–Sb system. *Intermetallics* 2003;11:1189–94.
- [4] Kuznetsov VL, Rowe DM. Solid solution formation in the — $Zn_4Sb_3Cd_4Sb_3$. *J Alloys Compd* 2004;372:103–6.
- [5] Ueno K, Yamamoto A, Noguchi T, Inoue T, Sodeoka S, Takazawa H, et al. Optimization of hot-press conditions of Zn_4Sb_3 for high thermoelectric performance I. Physical properties and thermoelectric performance. *J Alloys Compd* 2004;384:254–60.
- [6] Ur SC, Nash P, Kim Il H. Solid-state syntheses and properties of Zn_4Sb_3 thermoelectric materials. *J Alloys Compd* 2003;361:84–91.
- [7] Nylén J, Andersson M, Lidin S, Häussermann U. The structure of α - Zn_4Sb_3 : ordering of the phonon-glass thermoelectric materials β - Zn_4Sb_3 . *J Am Chem Soc* 2004;126:16306.
- [8] Cui JL, Xue HF, Xiu WJ, Yang W, Xu XB. Thermoelectric properties of Cu-doped p-type pseudo-binary $Cu_xBi_{0.5}Sb_{1.5-x}Te_3$ ($x = 0.05 \sim 0.4$) alloys prepared by spark plasma sintering. *Scr Mater* 2006;55:371–4.
- [9] Cui JL, Xiu WJ, Xue HF, Jiang L, Ying PZ. High thermoelectric properties of p-type pseudo-binary $(Cu_4Te_3)_x(Bi_{0.5}Sb_{1.5}Te_3)_{1-x}$ alloys prepared by spark plasma sintering. *J Appl Phys* 2007;101(123713):(1–4).
- [10] Cui JL, Xue HF, Xiu WJ. Thermoelectric properties of p-type pseudo-binary $(Ag_{0.365}Sb_{0.558}Te)_x(Bi_{0.5}Sb_{1.5}Te_3)_{1-x}$ ($x = 0 \sim 1.0$) alloys prepared by spark plasma sintering. *J Solid State Chem* 2006;179:3751–5.
- [11] Telkes M. The efficiency of thermoelectric generators. *I J Appl Phys* 1947;18:1116.
- [12] Shaver PJ, Blair J. Thermal and electronic transport properties of p-type ZnSb. *Phys Rev* 1966;141:649.
- [13] Zhang LT, Tsutsui M, Ito K, Yamaguchi M. Effects of ZnSb and Zn inclusions on the thermoelectric properties of β - Zn_4Sb_3 . *J Alloys Compd* 2003;358:252–6.
- [14] Li ML, editor. Concise handbook of chemical data. Beijing: Chemical Engineering Press; 2003. p. 6. [in Chinese].
- [15] Ueno K, Yamamoto A, Noguchi T, Li CH, Inoue T, Sodeoka S, et al. Effect of impurity oxygen concentration on the thermoelectric properties of hot-pressed Zn_4Sb_3 . *J Alloys Compd* 2006;417:259–63.

-
- [16] JCPDS-ICDD. JCPDS-International Center for Diffraction Data, Newtown Square, PA; 1999.
- [17] Kim SS, Yamamoto S, Aizawa T. Thermoelectric properties of anisotropy-controlled p-type Bi–Te–Sb system via bulk mechanical alloying and shear extrusion. *J Alloys Compd* 2004;375:107–13.
- [18] Venkatasubramanian R, Siivola E, Colpitts T, O B, Quinn. Thin-film thermoelectric devices with high room-temperature figures of merit. *Nature* 2001;413:597–602.